Structural Integrity Associates, Inc.®

CALCULATION PACKAGE

File No.: 1400669.322

Project No.: 1400669

Quality Program: ☒ Nuclear ☐ Commercial

PROJECT NAME:
Palisades Flaw Readiness Program for 1R24 NDE Inspection

CONTRACT NO.:
10426669

CLIENT:	**PLANT:**
Entergy Nuclear Operations, Inc.	Palisades Nuclear Plant

CALCULATION TITLE:
Cold Leg Bounding Nozzle Weld Residual Stress Analysis

Document Revision	Affected Pages	Revision Description	Project Manager Approval Signature & Date	Preparer(s) & Checker(s) Signatures & Date
0	1 - 38 A-1 - A-2 Computer Files	Initial Issue	Norman Eng NE 5/5/2015	Preparer: Wilson Wong WW 5/5/2015 Checkers: Minji Fong MF 5/5/2015 Gole Mukhim GSM 5/5/2015

Table of Contents

List of Tables

List of Figures

1.0 OBJECTIVE

The objective of this calculation package is to document the weld residual stress analysis for the bounding cold leg nozzle at the Palisades Nuclear Plant (Palisades). The bounding nozzle bounds the spray, drain, and charging nozzles discussed in a separate calculation package [1]. The weld residual stress analysis is based on the latest methodology and process developed by Structural Integrity Associates (SI).

2.0 TECHNICAL APPROACH

The finite element model is obtained from a previous finite element model (FEM) calculation package [1] and the weld residual stress analysis uses the latest weld residual stress analysis methodology developed by SI, using the ANSYS finite element analysis (FEA) program [3].

The residual stress analysis consists of a thermal pass followed by a stress pass where the temperature distribution time history from the thermal pass is used as temperature input into the stress pass to determine stresses. Stress results from the weld residual stress analysis are obtained and saved for future use to evaluate flaws which will be performed in a separate calculation package.

The finite element model includes all components in the post-nozzle installation stage because new elements cannot be added during an ANSYS analysis. Since all the weld elements need to be included in the initial model, the element "birth and death" technique in ANSYS is used to initially deactivate the weld elements, with elements corresponding to the active weld segment reactivated at the melting temperature, thus simulating the weld metal deposition.

2.1 Material Properties

The weld residual stress analysis performed in this calculation uses the material properties specifically developed in a separate calculation package for weld residual stress analyses [2]. Per the material designation used in the FEM calculation [1], the following materials are used:

- SA-516 Grade 70: Cold leg base metal
- ER308L: Cold leg cladding (typical weld metal for Type 304)
- Alloy 82/182: Boss weld and ID patch weld
- Alloy 600 (SB-166): Nozzle

The material properties are reproduced in Table 1 through Table 8.

2.2 Finite Element Model for Weld Residual Stress Analysis

The finite element model for the analysis was developed in a previous FEM calculation [1], which was created using the ANSYS finite element analysis software package [3]. The base finite element model

for the weld residual stress analysis is meshed with 8-node solid elements (SOLID185) in ANSYS. This finite element model is shown in Figure 1.

2.3 Welding Simulation

The FEA for predicting the weld residual stresses is performed as a continuous analysis so that the load history from the cladding is carried over to the nozzle-to-pipe weld and the ID patch weld. Specifically, the residual stresses and strains at the end of a weld pass are used as initial conditions at the start of the next weld pass.

The procedures for this complex multi-step simulation are encoded in ANSYS Parametric Design Language (APDL) macros which utilize elastic-plastic material behavior and elements with large deformation capability to predict the residual stresses due to the various welding processes.

2.4 Heat Inputs

The deposition of the weld metal is simulated by imposing a heat generation function on the elements of the FEM representing the active weld, which is applied as a volumetric body heat generation rate. The amount of equivalent heat input energy, Q (in terms of kJ/inch), is determined from the welding parameters.

Since the welding parameters for the welds are not available, a typical heat input of 28 kJ/inch, with an overall heat efficiency of 0.8, is assumed for all the welds. The heat efficiency represents a "composite" value reflecting the concepts of arc efficiency, melting efficiency, etc., and is an optimum value to produce reasonable heat penetration in the analysis.

The APDL macros automatically calculate the appropriate time intervals for the thermal pass to ensure that sufficient heat penetration is achieved, the required interpass temperature between weld passes is met, and a reasonable overall temperature distribution within the finite element model is achieved. The resulting temperature time history is then imported into the stress pass in order to calculate the residual stresses due to the thermal cycling of the weld elements using nonlinear, elastic-plastic load/unload stress reversal relations.

The following summarizes the welding parameters used in the analysis:

- Interpass temperature = 350°F [4]
- Melting temperature = 2500°F (See Section 3.0)
- Reference temperature = 70°F (See Section 3.0)
- Heat input for all welds = 28 kJ/in (See Section 3.0)
- Heat efficiency for all welds = 0.8 (See Section 3.0)
- Inside/Outside heat transfer coefficient = 5 Btu/hr-ft^2-°F (See Section 3.0)
- Inside/Outside temperature = 70°F (See Section 3.0)

2.5 Creep Properties

Strain relaxation due to creep at high temperature is considered in the post-weld heat treatment (PWHT) step of the analysis. In general, creep becomes significant at temperatures above 800°F; thus, creep behavior under 800°F will not be considered in this analysis. The creep properties listed in Table 9 are determined in the previous FEM calculation [1].

2.6 Mechanical Boundary Conditions

The mechanical boundary conditions for the stress analysis are symmetric boundary conditions at the symmetry planes of the model, axial displacement restraint at the end of the nozzle, and axial displacement coupling at the end of the cold leg piping, as shown in Figure 2.

3.0 ASSUMPTIONS

The following assumptions are used in the analyses:

- The cold leg cladding material is assumed to be ER308L, which is a typical weld metal for Type 304 stainless steel cladding.
- The metal melting temperature is assumed to be 2500°F, which is the temperature point where the strength of the material is set to near zero [2].
- The analysis is performed with a reference temperature of 70°F.
- The exposed surface of the model is subject to a typical ambient air cooling convection film coefficient of 5 Btu/hr-ft^2-°F at a bulk temperature of 70°F. The exposed surfaces are defined as the exterior surfaces of the model excluding the symmetry planes and the far ends of the modeled piping and nozzle.
- Since the welding parameters for the welds are not available, a typical heat input of 28 kJ/in, with an overall heat efficiency of 0.8, is assumed for all of the welds.
- The focus of this analysis is the residual stresses in the nozzle boss weld region, while the interaction between the clad buildup and the cold leg base metal has secondary effects on the region of interest. Therefore, the clad is assumed to be fully deposited in a single one-layer pass.
- The boss weld is represented by a 40-bead process, as shown in Figure 3, with each bead represented by a one pass "bead ring" nugget. This approach is a common and acceptable industry practice when information regarding the bead start/stop position and sequencing are unknown.
- Similarly, the ID patch weld is represented by a 6-bead process, as shown in Figure 4, with each bead represented by a one pass "bead ring" nugget.
- For model simplification, the penetration hole is present during the deposition of the clad material. This is acceptable since any localized stress with or without the hole would have negligible impact on the final results.

- For convenience, the modeled ID patch weld has the same geometry as the backing ring for the boss weld.
- Additional assumptions on PWHT are discussed in Section 4.4.

4.0 WELD RESIDUAL STRESS ANALYSIS

The weld residual stress analysis consists of a thermal analysis to determine the temperature distribution followed by a stress analysis to determine the resulting stresses. The analytical sequence described below is used in the finite element analysis, followed by detailed discussions of the steps in Sections 4.1 through 4.6:

1. Deposit cladding on cold leg pipe inside (ID) surface.
2. Install nozzle, backing ring, and deposit boss weld.
3. Remove backing ring and deposit ID patch weld.
4. Post-weld heat treatment, including creep effects based upon experimental data per Table 9.
5. Subject the configuration to a hydrostatic test.
6. Impose five cycles of "shake down" with normal operating temperature and pressure to stabilize the residual stress fluctuations due to stress redistribution caused by normal operating loads.

4.1 Cold leg Cladding

The clad material is typically welded onto the inside surface of the cold leg pipe, and the nominal thickness of the clad is thicker than the typical thickness for a single weld layer used in the process. However, the focus of this analysis is on the as-welded residual stresses, while the interaction between the clad buildup and the base material during the many actual weld passes is not of interest. Therefore, the clad is assumed to be fully deposited in a single pass.

At this step, only the cold leg pipe base metal elements and clad material elements are active; all other components are deactivated during the analysis. At the end of the cladding application, the entire model is cooled to 70°F before the application of the boss weld.

4.2 Boss Weld

The boss weld connects the nozzle boss to the cold leg piping. As shown in Figure 3, the weld is composed of 40 nuggets deposited in 20 weld layers. In the absence of detailed weld fabrication information, a weld sequence is assumed based on standard welding practice at the time of fabrication. In particular, for every layer, the first nugget is deposited on the cold leg side, the second nugget on the nozzle side.

At this step, the nozzle elements and backing ring elements are reactivated, and the boss weld nuggets are reactivated sequentially to simulate the welding process. The preheat temperature of the boss weld is 250°F [4]. At the end of the boss weld, the entire model is cooled to 70°F before the application of the ID patch weld.

4.3 ID Patch Weld

The final weld step is to add the ID patch weld, which replaces the backing ring. As seen in Figure 4, the ID patch weld is composed of 6 nuggets deposited in 2 layers.

At this step, the backing ring is first deactivated to allow the residual stresses to redistribute, and the ID patch weld nuggets are reactivated sequentially to simulate the welding process. The preheat temperature of the ID patch weld is 250°F [4]. At the end of the ID patch weld, the entire model is cooled to 70°F before the application of the PWHT.

4.4 Post-weld Heat Treatment

PWHT is assumed to be performed as per the following procedure outlined in Article N-532 of the ASME Code, Section III [7] and the welding procedure [4] for welding on material group P-1:

1. Heat welded piping component to 1150°F at a heating rate of 400°F per hour divided by the maximum metal thickness (133° per hour for 3 inch thick cold leg) [7, Article N-532.3 (2)].
2. Hold at temperature for approximately 3 hours (1hr/in of weld thickness) [7, Table N-532.3].
3. Allow to cool to 600°F at a cooling rate of 500°F per hour divided by the maximum metal thickness (167° per hour for 3 inch thick cold leg) at temperatures above 600°F [7, Article N-532.3 (5)].
4. Air-cool from 600°F to ambient [7, Article N-532.3 (5)].
5. A steady state load step is imposed at the end of the PWHT process.

During the PWHT, creep behavior is activated for time steps with the maximum temperature above 800°F. At the end of the PWHT, the entire model is cooled 70°F before the application of the hydrostatic test.

4.5 Hydrostatic Test

A hydrostatic test pressure of 3110 psig (3125 psia) and a temperature of 400°F [8, page 9] are applied after the welding. The pressure is applied on the ID surfaces of the cold leg pipe and nozzle. An end-cap load, $P_{end\text{-}cap\text{-}cl}$, is applied at the free end of the cold leg piping. This is calculated based on the following expression:

$$P_{end\text{-}cap\text{-}cl} = \frac{P \cdot r_{inside\_cl}^{2}}{\left(r_{outside\_cl}^{2} - r_{inside\_cl}^{2}\right)} =$$

where,

P	= Hydrostatic test pressure (ksi)
$P_{end\text{-}cap\text{-}cl}$	= End cap pressure on cold leg pipe end (ksi)
r_{inside_cl}	= Inside radius of cold leg pipe (in)
$r_{outside\_cl}$	= Outside radius of cold leg pipe (in)

The applied pressure loads on the model are shown in Figure 5.

4.6 Five Normal Operating Cycles (NOC)

After the hydrostatic test, the assembled configuration is put into service and subjected to 5 cycles of shake down to stabilize the as-welded residual stresses. This step involves simultaneously ramping the model from zero-load to steady-state conditions at normal operating temperature and pressure then back to steady-state at 70°F and no pressure five times.

The applied operating pressure and temperature is 2085 psig (2100 psia) and 537°F [9]. The temperature is assumed to be uniform throughout the components and operating pressure is applied as an internal pressure on the ID surface, with corresponding end-cap pressure calculated using the equation in the previous section. The term "P" is replaced by the operating pressure in the expression.

5.0 RESULTS OF WELD RESIDUAL STRESS ANALYSIS

The ANSYS input files and computer output files for the analyses are listed in Appendix A.

5.1 Welding Temperature Contours

The maximum temperature prediction contours for each weld are created using macro **MapTemp.mac**. This type of contour plot is also called a "fusion boundary" plot because it provides an overview of the maximum temperature on each node throughout the thermal transient for each welding process. The plots are useful in visualizing the melting of weld metal and the extent of heat penetration.

The predicted fusion boundary contours for the cladding, boss weld, and ID patch weld are shown in Figure 6, Figure 7, and Figure 8, respectively. The purple color in the plots represents elements at melting temperature (>2500°F); the plots show complete melting of the weld metal for each weld and slight melting of the base metal along the weld interface.

5.2 PWHT Temperature Results

Figure 9 plots the inside surface temperature curve for the PWHT process. It shows the linear 133°F/hour heating rate, three hours (180 minutes) hold time at 1150°F, 167°F/hour cooling rate at temperature above 600°F, and the air cooling to room temperature of 70°F.

5.3 Residual Stress Results

Figure 10 plots the von Mises residual stresses after welding is complete, but before PWHT. It shows extensive residual stresses of greater than 66 ksi in the weld material. However, as shown in Figure 11, after the PWHT the residual stresses in the weld have relaxed significantly, to below 41 ksi, but the residual stresses in the cladding remain essentially unchanged.

To further investigate the effects of the PWHT, before and after PWHT residual stresses are extracted along the two through-wall paths shown in Figure 12. The through-wall residual stresses are compared in Figure 13, and it shows that there is little to no stress reduction in the clad material, while there is significant stress reduction in the pipe base metal.

The PWHT results from the FEA trend comparably well with the data in EPRI report TR-105697 [10], which contains a comparable through-wall clad residual stress distribution based on experimental measurements, as shown in Figure 14. The experimental measurements were for a low alloy steel vessel with a Type 304 stainless steel clad. The data shows tensile hoop stress through the clad thickness and the base metal near the clad interface, but the hoop stress drops rapidly to compressive values at farther distances from the clad.

Figure 15 depicts the predicted von Mises residual stresses after the hydrostatic test. It shows an insignificant reduction in maximum stress when compared to the post-PWHT step: 73.74 ksi (Figure 15) versus 73.75 ksi (Figure 11), while the overall stress contour remains essentially the same.

Figure 16 and Figure 17 depicts the combined weld residual plus operating radial and hoop stresses, respectively, at the fifth stabilization NOC cycle. The stress results at this step are used in the fracture mechanics evaluations.

6.0 CONCLUSIONS

Finite element residual stress analysis has been performed on the bounding cold leg nozzle boss weld at Palisades. Stresses at normal operating conditions combined with residual stresses have been obtained and saved for future use. The stress results will be used in a separate calculation to determine crack growth.

7.0 REFERENCES

1. SI Calculation No. 1400669.320, Rev. 0, "Finite Element Model Development for the Cold Leg Drain, Spray, and Charging Nozzles."
2. SI Calculation No. 0800777.307, Rev. 5, "Material Properties for Residual Stress Analyses, Including MISO Properties Up To Material Flow Stress."
3. ANSYS Mechanical APDL and PrepPost, Release 14.5 (w/ Service Pack 1), ANSYS, Inc., September 2012.
4. Combustion Engineering Welding Procedure No. MA-41, Rev.0, SI File No. 1400669.204.
5. "Steels for Elevated Temperature Service," United States Steel Co., 1949.
6. Publication SMC-027, "Inconel Alloy 600," Special Metals Corp., 2004, SI File 0800777.211.
7. ASME Boiler and Pressure Vessel Code, Section III, 1965 Edition with Addenda through Winter 1966.
8. Combustion Engineering Specification No. 0070P-006, Rev. 2, "Engineering Specification for Primary Coolant Pipe and Fittings," SI File No. 1300086.203.
9. Palisades Design Input Record, "Palisades Alloy 600 Flaw Eval DIR 3-4-15 Rev1.pdf," SI File No. 1400669.201.
10. EPRI Report No. TR-105697, "BWR Reactor Pressure Vessel Shell Weld Inspection Recommendations (BWRVIP-05)," September 1995.

Table 1: Elastic Properties for SA-516 Grade 70 (≤4" Thick)

Temperature (°F)	Young's Modulus ($x10^3$ ksi)	Mean Thermal Expansion ($x10^{-6}$ in/in/°F)	Thermal Conductivity (2) (Btu/min-in-°F)	Specific Heat (2) (Btu/lb-°F)
70	29.5	6.4	0.0488	0.103
500	27.3	7.3	0.0410	0.128
700	25.5	7.6	0.0369	0.138
1100	18.0	8.2	0.0290	0.171
1500	5.0	8.6	0.0218	0.198
2500	0.1	9.5	0.0014	0.204
2500.1	–	0.0	–	–

Notes:
1. All values per [2].
2. Density (ρ) = 0.283 lb/in^3 [2], assumed temperature independent.
3. Poisson's Ratio (υ) = 0.3 [2], assumed temperature independent.

Table 2: Elastic Properties for ER308L

Temperature (°F)	Young's Modulus ($x10^3$ ksi)	Mean Thermal Expansion ($x10^{-6}$ in/in/°F)	Thermal Conductivity (2) (Btu/min-in-°F)	Specific Heat (2) (Btu/lb-°F)
70	28.3	8.5	0.0119	0.116
500	25.8	9.7	0.0151	0.131
700	24.8	10.0	0.0164	0.135
1100	22.1	10.5	0.0189	0.140
1500	18.1	10.8	0.0213	0.145
2500	0.1	11.5	0.0292	0.159
2500.1	–	0.0	–	–

Notes:
1. All values per [2].
2. Density (ρ) = 0.283 lb/in^3 [2], assumed temperature independent.
3. Poisson's Ratio (υ) = 0.3 [2], assumed temperature independent.

Table 3: Elastic Properties for Alloy 600

Temperature (°F)	Young's Modulus ($x10^3$ ksi)	Mean Thermal Expansion ($x10^{-6}$ in/in/°F)	Thermal Conductivity (2) (Btu/min-in-°F)	Specific Heat (2) (Btu/lb-°F)
70	31.0	6.8	0.0119	0.108
500	29.0	7.6	0.0147	0.120
700	28.2	7.9	0.0161	0.125
1100	25.9	8.4	0.0192	0.139
1500	23.1	9.0	0.0222	0.148
2500	0.1	10.0	0.0306	0.177
2500.1	–	0.0	–	–

Notes:
1. All values per [2].
2. Density (ρ) = 0.300 lb/in^3 [2], assumed temperature independent.
3. Poisson's Ratio (υ) = 0.29 [2], assumed temperature independent.

Table 4: Elastic Properties for Alloy 82/182

Temperature (°F)	Young's Modulus ($x10^3$ ksi)	Mean Thermal Expansion ($x10^{-6}$ in/in/°F)	Thermal Conductivity (2) (Btu/min-in-°F)	Specific Heat (2) (Btu/lb-°F)
70	31.0	6.8	0.0119	0.108
500	29.0	7.6	0.0147	0.120
700	28.2	7.9	0.0161	0.125
1100	25.9	8.4	0.0192	0.139
1500	23.1	9.0	0.0222	0.148
2500	0.1	10.0	0.0306	0.177
2500.1	–	0.0	–	–

Notes:
1. All values per [2].
2. Density (ρ) = 0.300 lb/in^3 [2], assumed temperature independent.
3. Poisson's Ratio (υ) = 0.29 [2], assumed temperature independent.

Table 5: Stress-Strain Curves for SA-516 Grade 70 (≤4" Thick)

Temperature (°F)	Strain (in/in)	Stress (ksi)
70	0.00128814	38.000
	0.00187809	42.000
	0.00257329	46.000
	0.00381110	50.000
	0.00600383	54.000
500	0.00113553	31.000
	0.00142679	35.875
	0.00183954	40.750
	0.00261139	45.625
	0.00415246	50.500
700	0.00106667	27.200
	0.00132412	32.550
	0.00166876	37.900
	0.00228121	43.250
	0.00354341	48.600
1100	0.00116667	21.000
	0.05116163	22.125
	0.05915444	23.250
	0.06794123	24.375
	0.07755935	25.500
1500	0.00300000	15.000
	0.16717493	15.125
	0.16992011	15.250
	0.17268761	15.375
	0.17547742	15.500
2500[2]	0.01000000	1.000
	0.10961239	1.125
	0.12781277	1.250
	0.14689940	1.375
	0.16683167	1.500

Notes:
1. All values per [2].
2. Values at 2500°F assumed arbitrarily small values for convergence stability.

Table 6: Stress-Strain Curves for ER308L

Temperature (°F)	Strain (in/in)	Stress (ksi)
70	0.00203180	57.500
	0.02471351	61.563
	0.03107296	65.625
	0.03861377	69.688
	0.04747167	73.750
500	0.00140089	36.143
	0.00714793	40.250
	0.01065407	44.357
	0.01558289	48.464
	0.02233857	52.571
700	0.00132488	32.857
	0.00477547	37.125
	0.00743595	41.393
	0.01143777	45.661
	0.01727192	49.929
1100	0.00121913	26.943
	0.00264833	30.138
	0.00404100	33.332
	0.00634529	36.527
	0.01005286	39.721
1500	0.00117995	21.357
	0.05352064	21.563
	0.05610492	21.768
	0.05878975	21.973
	0.06157807	22.179
2500[2]	0.01000000	1.000
	0.10961239	1.125
	0.12781277	1.250
	0.14689940	1.375
	0.16683167	1.500

Notes:
1. All values per [2].
2. Values at 2500°F assumed arbitrarily small values for convergence stability.

Table 7: Stress-Strain Curves for Alloy 600

Temperature (°F)	Strain (in/in)	Stress (ksi)
70	0.00157419	48.800
	0.01658847	55.300
	0.02343324	61.800
	0.03212188	68.300
	0.04291703	74.800
500	0.00152069	44.100
	0.01539220	50.338
	0.02210610	56.575
	0.03072476	62.813
	0.04153277	69.050
700	0.00152128	42.900
	0.01634485	49.000
	0.02334760	55.100
	0.03227153	61.200
	0.04338643	67.300
1100	0.00155985	40.400
	0.02275193	44.475
	0.03004563	48.550
	0.03888203	52.625
	0.04943592	56.700
1500	0.00092641	21.400
	0.08827666	22.475
	0.09785101	23.550
	0.10796967	24.625
	0.11863796	25.700
2500[2]	0.01000000	1.000
	0.10961239	1.125
	0.12781277	1.250
	0.14689940	1.375
	0.16683167	1.500

Notes:
1. All values per [2].
2. Values at 2500°F assumed arbitrarily small values for convergence stability.

Table 8: Stress-Strain Curves for Alloy 82/182

Temperature (°F)	Strain (in/in)	Stress (ksi)
70	0.00179032	55.500
	0.03456710	60.113
	0.04292837	64.725
	0.05257245	69.338
	0.06359421	73.950
500	0.00164483	47.700
	0.02976152	52.313
	0.03809895	56.925
	0.04790379	61.538
	0.05929946	66.150
700	0.00159574	45.000
	0.02849157	49.538
	0.03680454	54.075
	0.04663682	58.613
	0.05812078	63.150
1100	0.00159073	41.200
	0.03568855	44.488
	0.04402702	47.775
	0.05360088	51.063
	0.06449835	54.350
1500	0.00106494	24.600
	0.11812735	25.325
	0.12540227	26.050
	0.13290814	26.775
	0.14064577	27.500
2500[2]	0.01000000	1.000
	0.10961239	1.125
	0.12781277	1.250
	0.14689940	1.375
	0.16683167	1.500

Notes:
1. All values per [2].
2. Values at 2500°F assumed arbitrarily small values for convergence stability.

Table 9: Creep Properties

Material	Temperature (°F)	Creep Strength (ksi)		*A* (ksi/hr)	*n*
		σ_1 (0.0001%/hr)	σ_2 (0.00001%/hr)		
SA-516 Gr. 70 (Based on carbon steel) Per [5]	800	19.0	12.4	1.26E-13	5.40
	900	9.0	6.7	3.59E-14	7.80
	1000	3.5	2.8	2.43E-12	10.32
	1100	1.4	0.8	2.50E-07	4.11
ER308L (Based on Type 304) Per [5]	800	33.4	25.0	7.73E-19	7.95
	900	24.0	17.6	5.67E-17	7.42
	1000	17.6	11.5	1.82E-13	5.41
	1100	11.5	7.1	8.62E-12	4.77
Alloy 600 Alloy 82/182 (Based on Alloy 600) Per [6]	800	40.0	30.0	1.50E-19	8.00
	900	28.0	18.0	2.87E-14	5.21
	1000	12.5	6.1	3.02E-10	3.21
	1100	6.8	3.4	1.72E-09	3.32

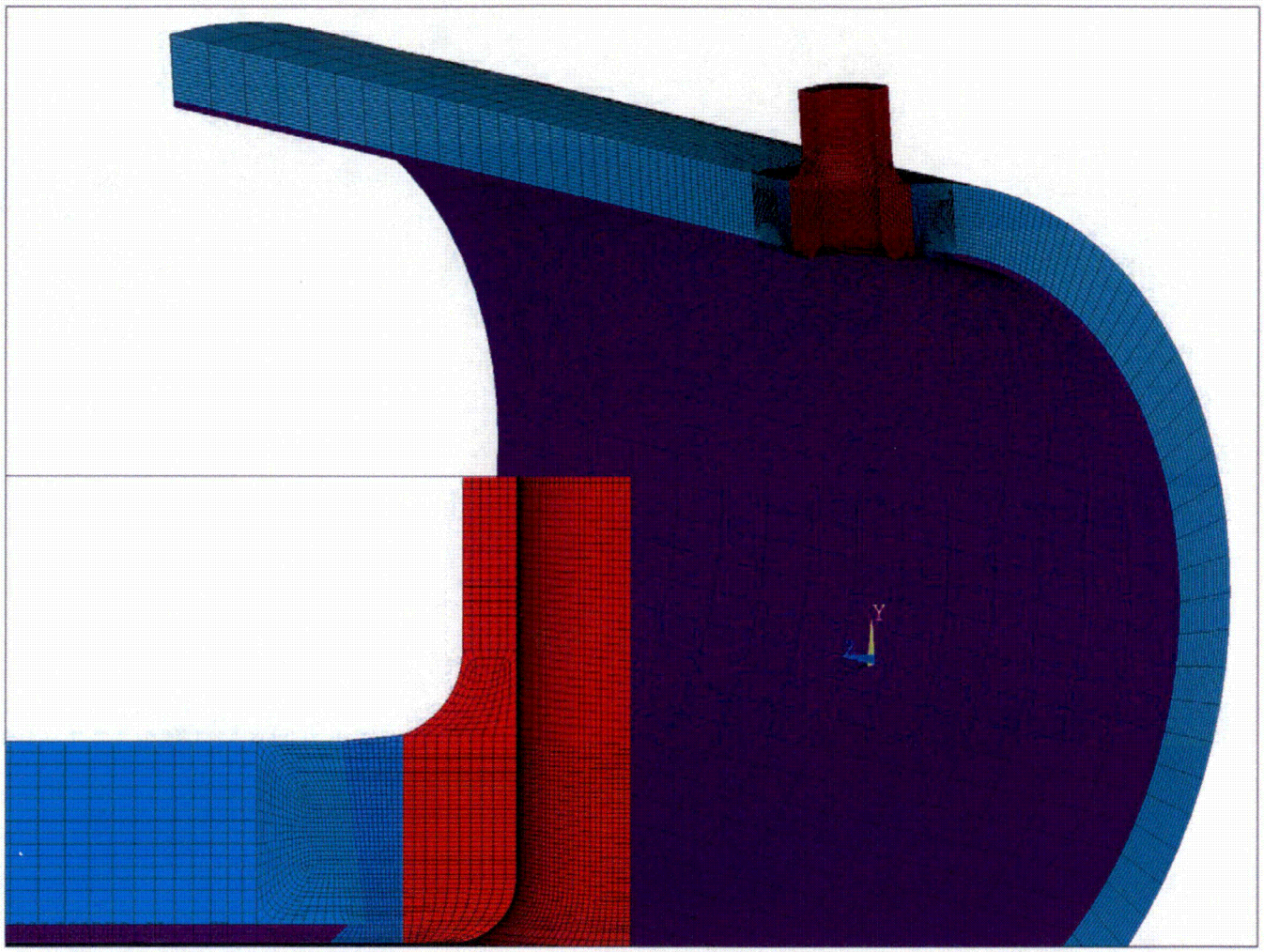

Figure 1: Finite Element Model for Residual Stress Analysis

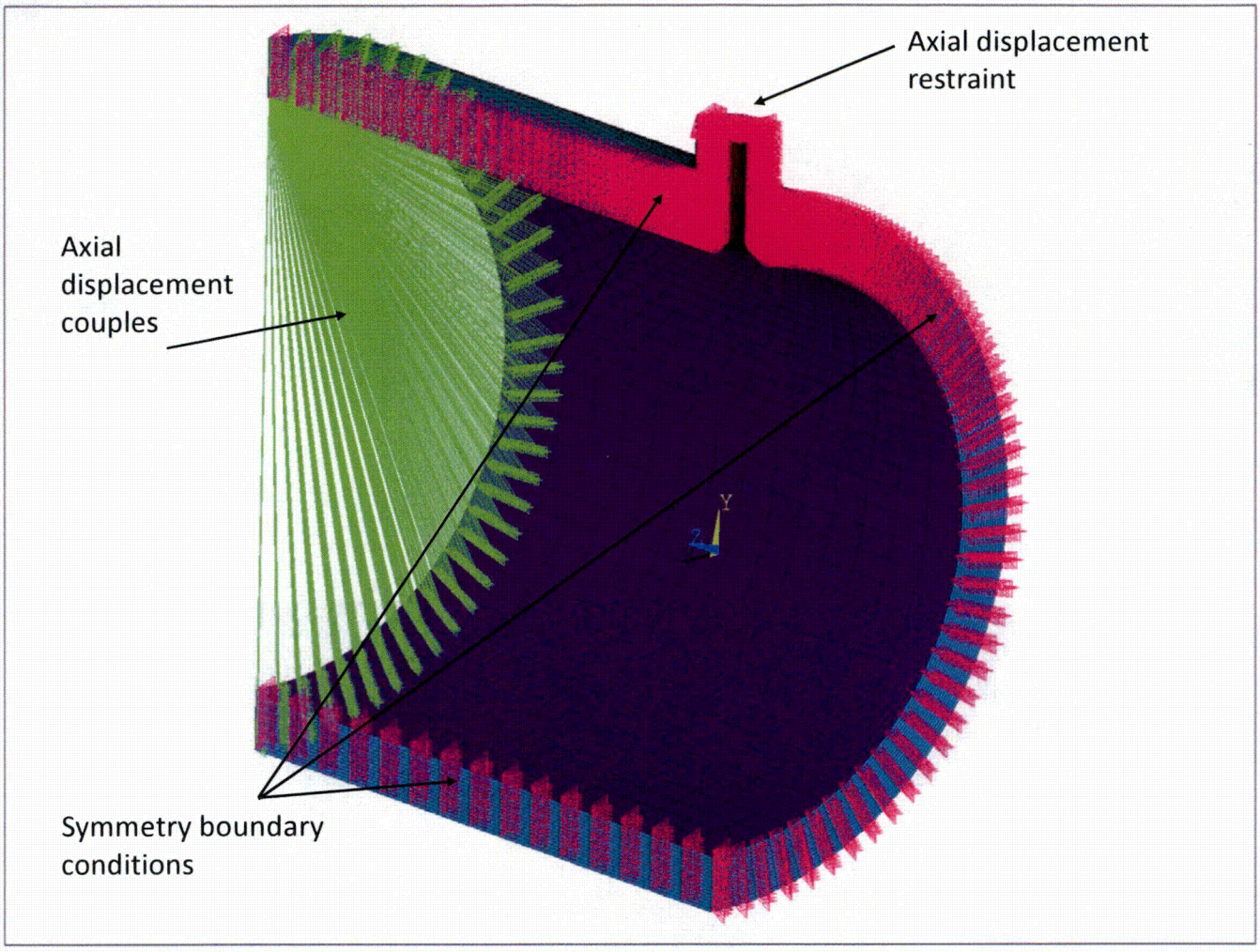

Figure 2: Applied Mechanical Boundary Conditions

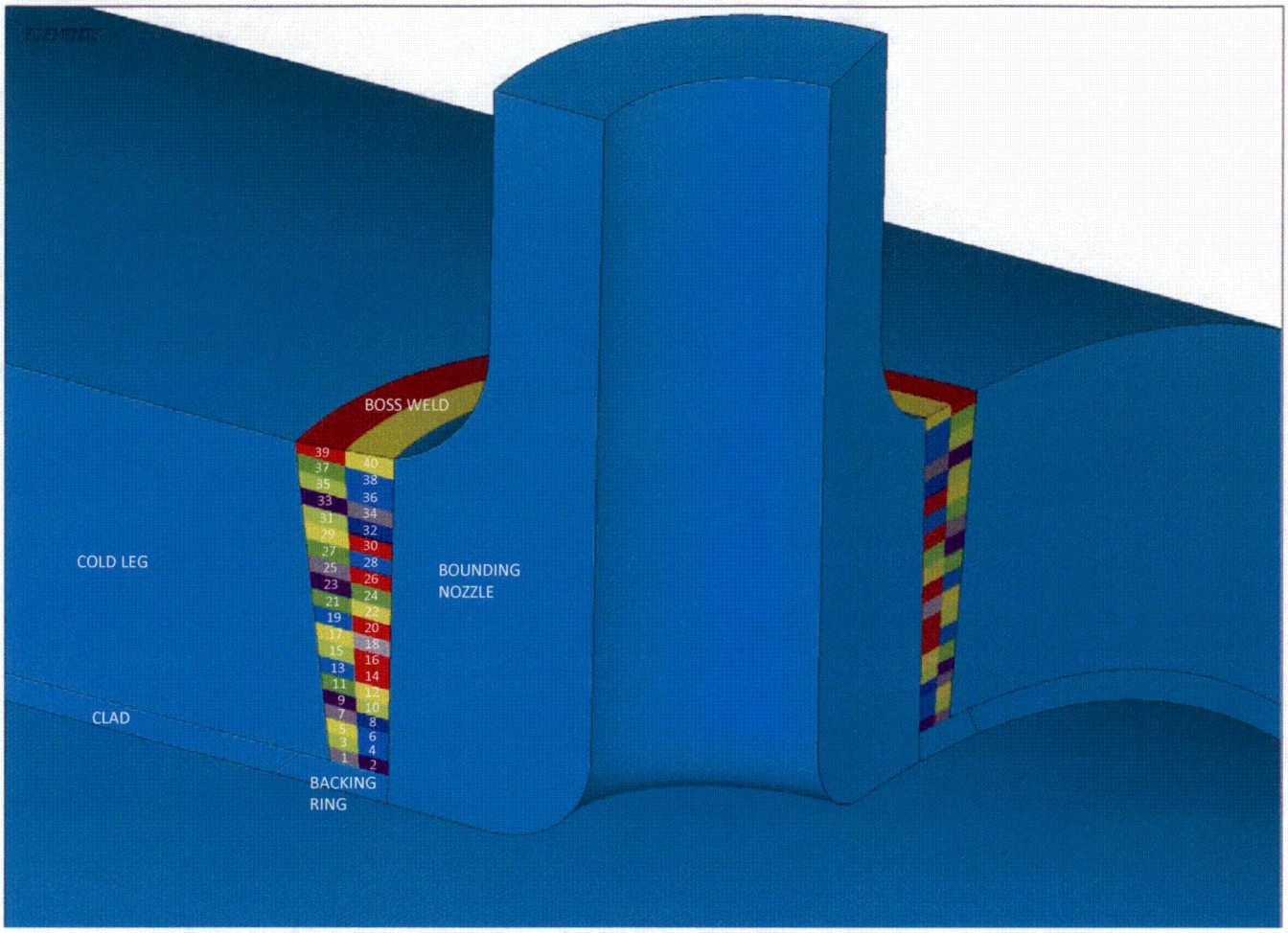

Figure 3: Weld Nugget Definitions for the Boss Weld

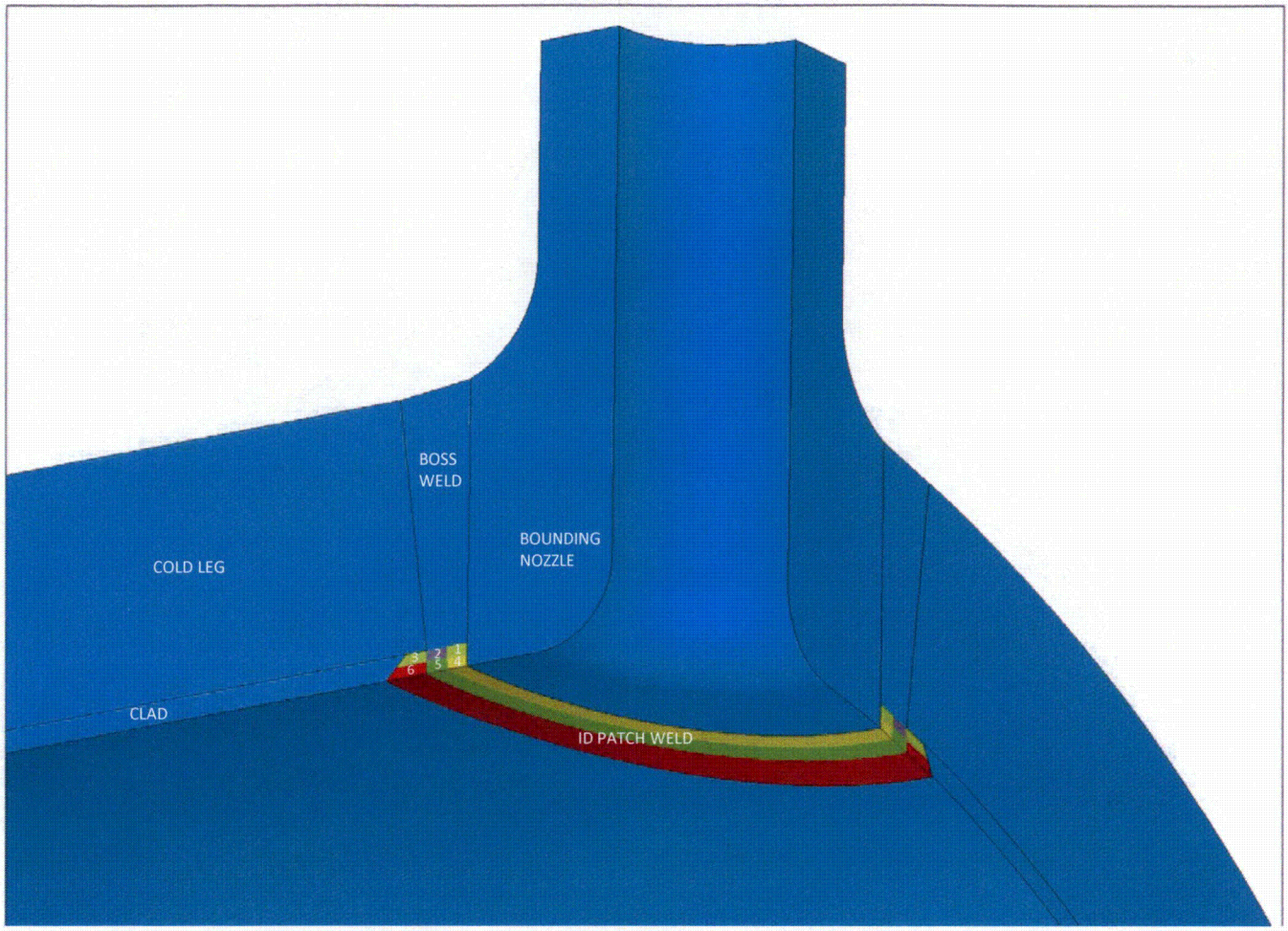

Figure 4: Weld Nugget Definitions for the ID Patch Weld

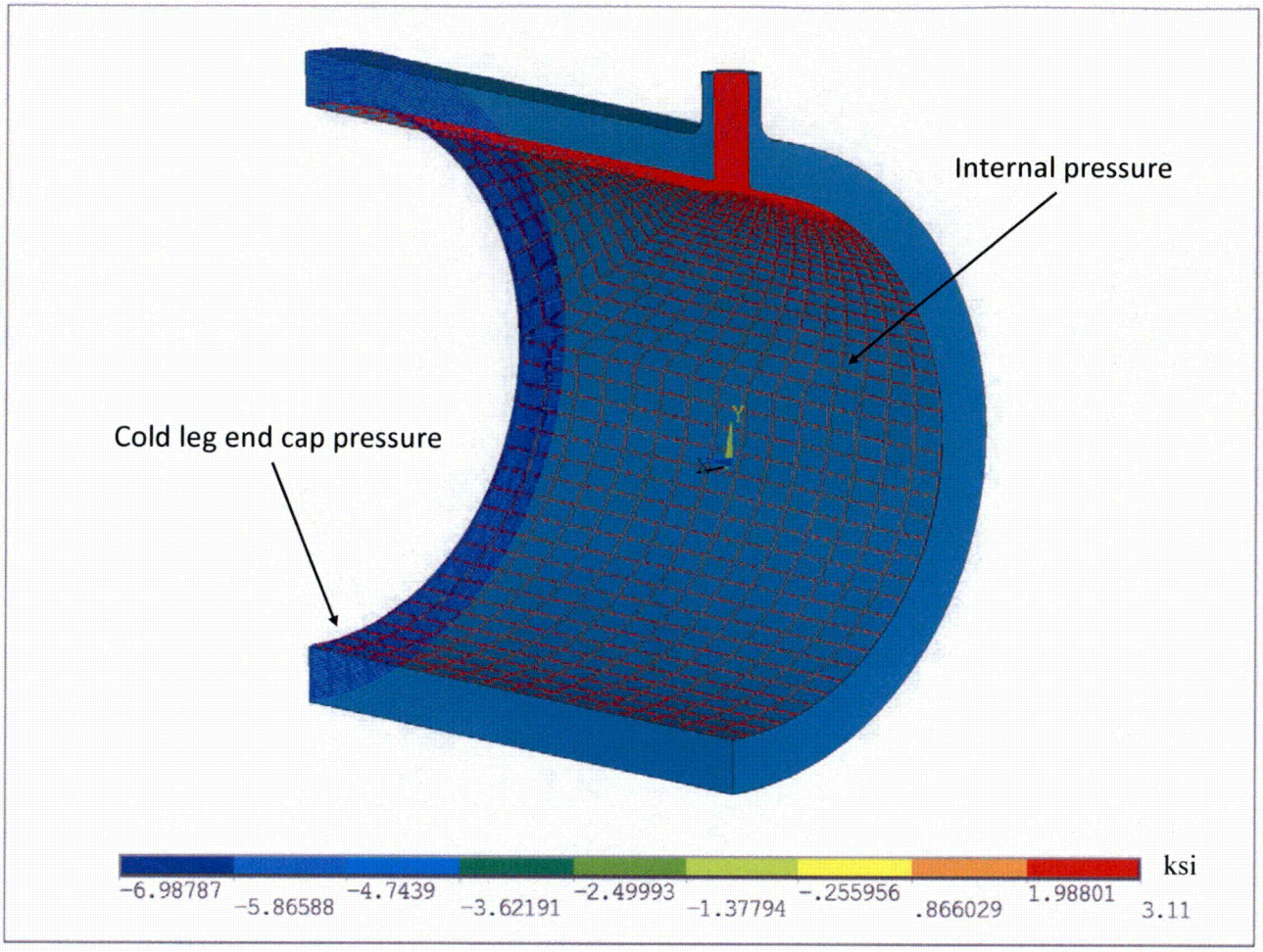

Figure 5: Applied Hydrostatic Test Pressure and Corresponding End Cap Pressure Loads

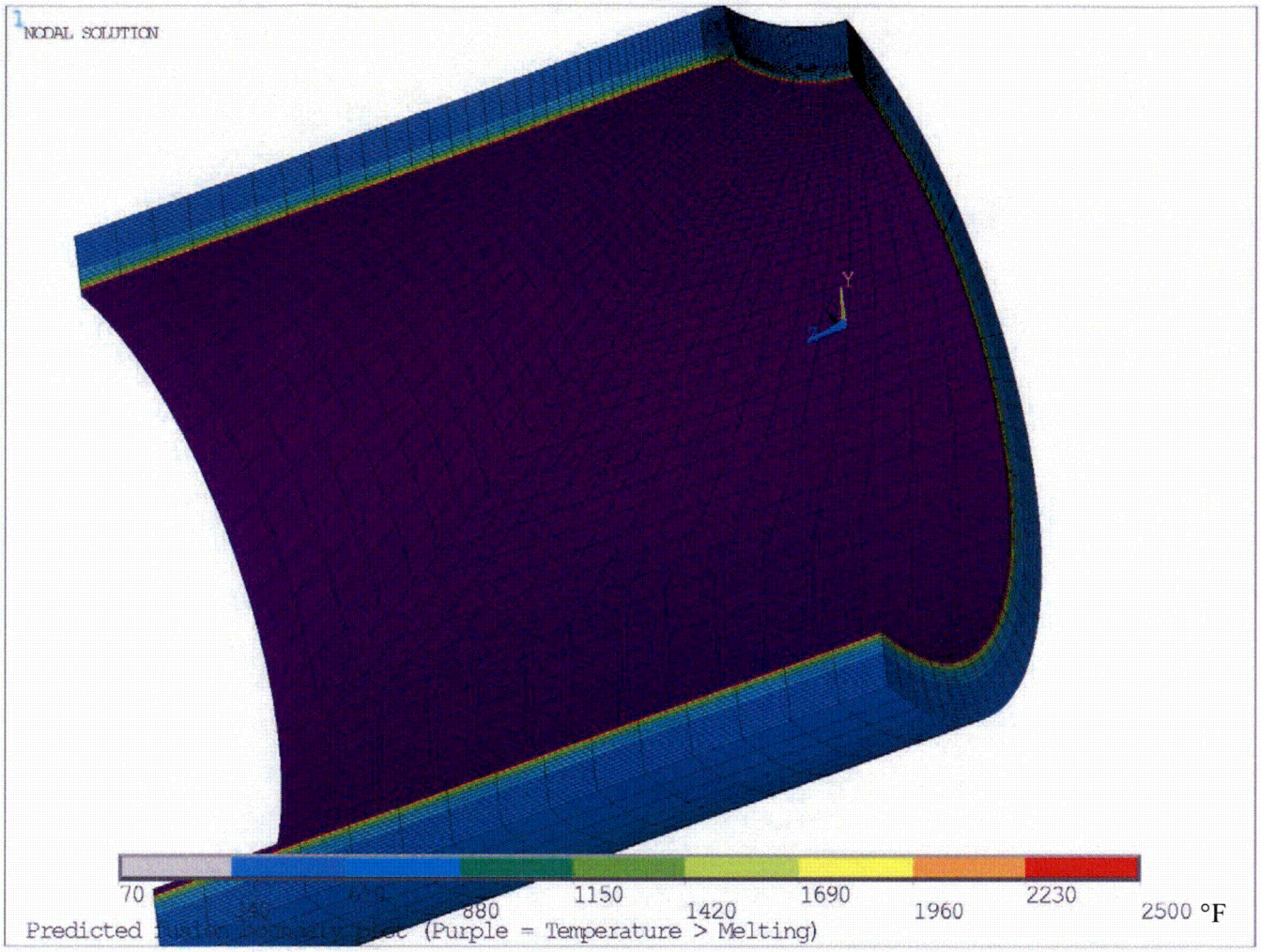

Figure 6: Predicted Fusion Boundary Plot for Cladding

(Note: Purple = Temperature > Melting Temperature of 2500°F)

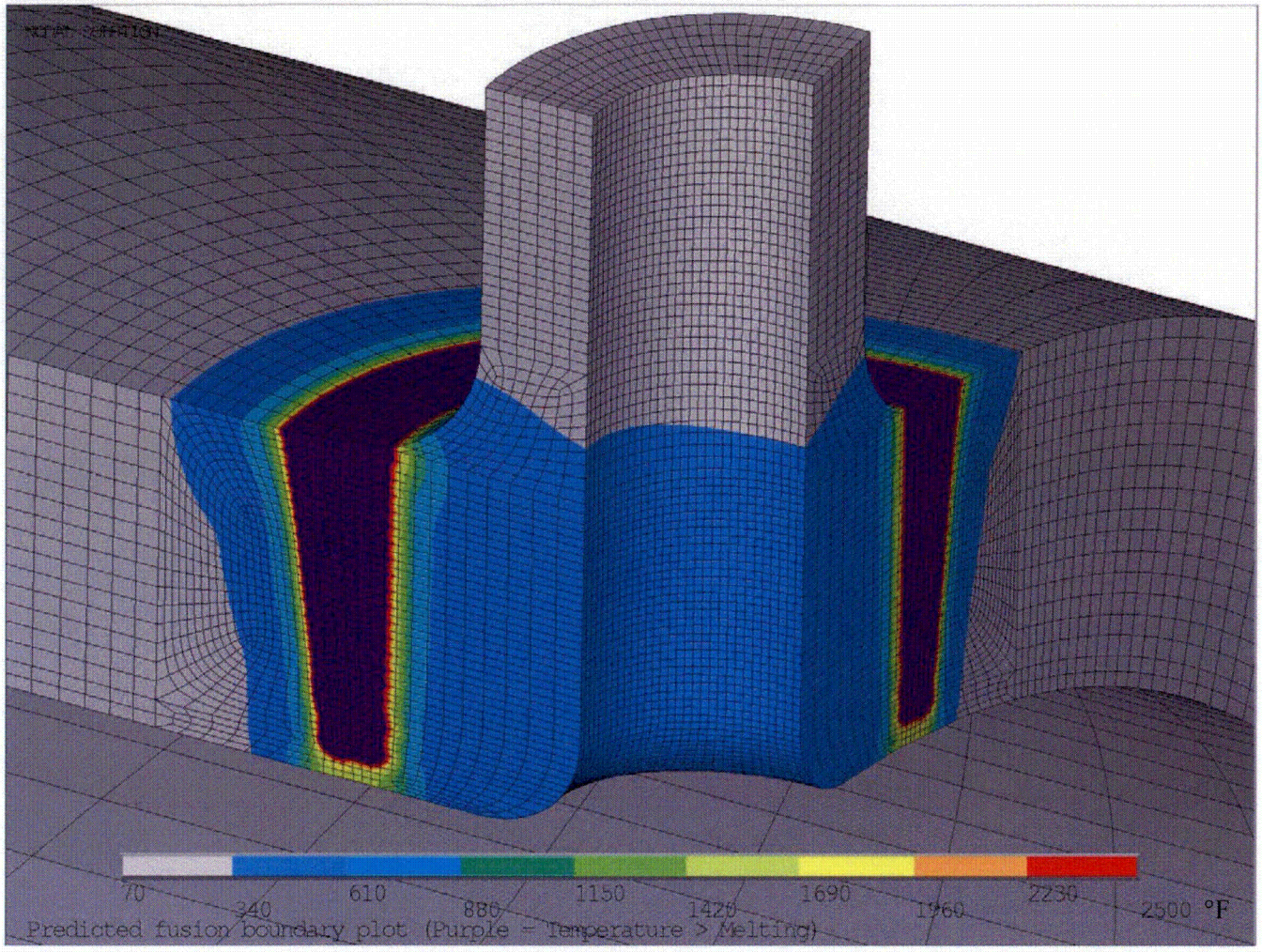

Figure 7: Predicted Fusion Boundary Plot for Boss Weld

(Note: Purple = Temperature > Melting Temperature of 2500°F)

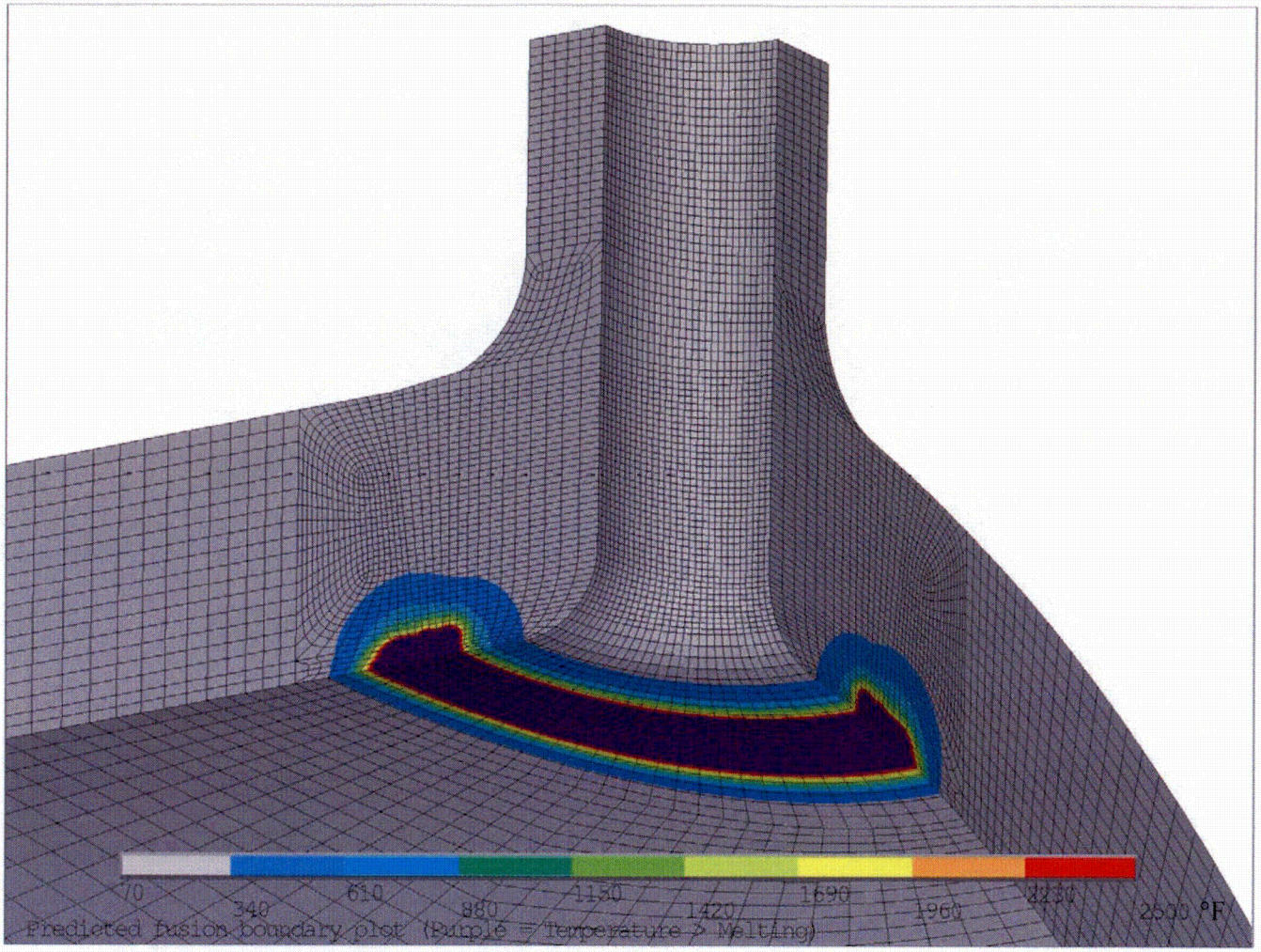

Figure 8: Predicted Fusion Boundary Plot for ID Patch Weld

(Note: Purple = Temperature > Melting Temperature of 2500°F)

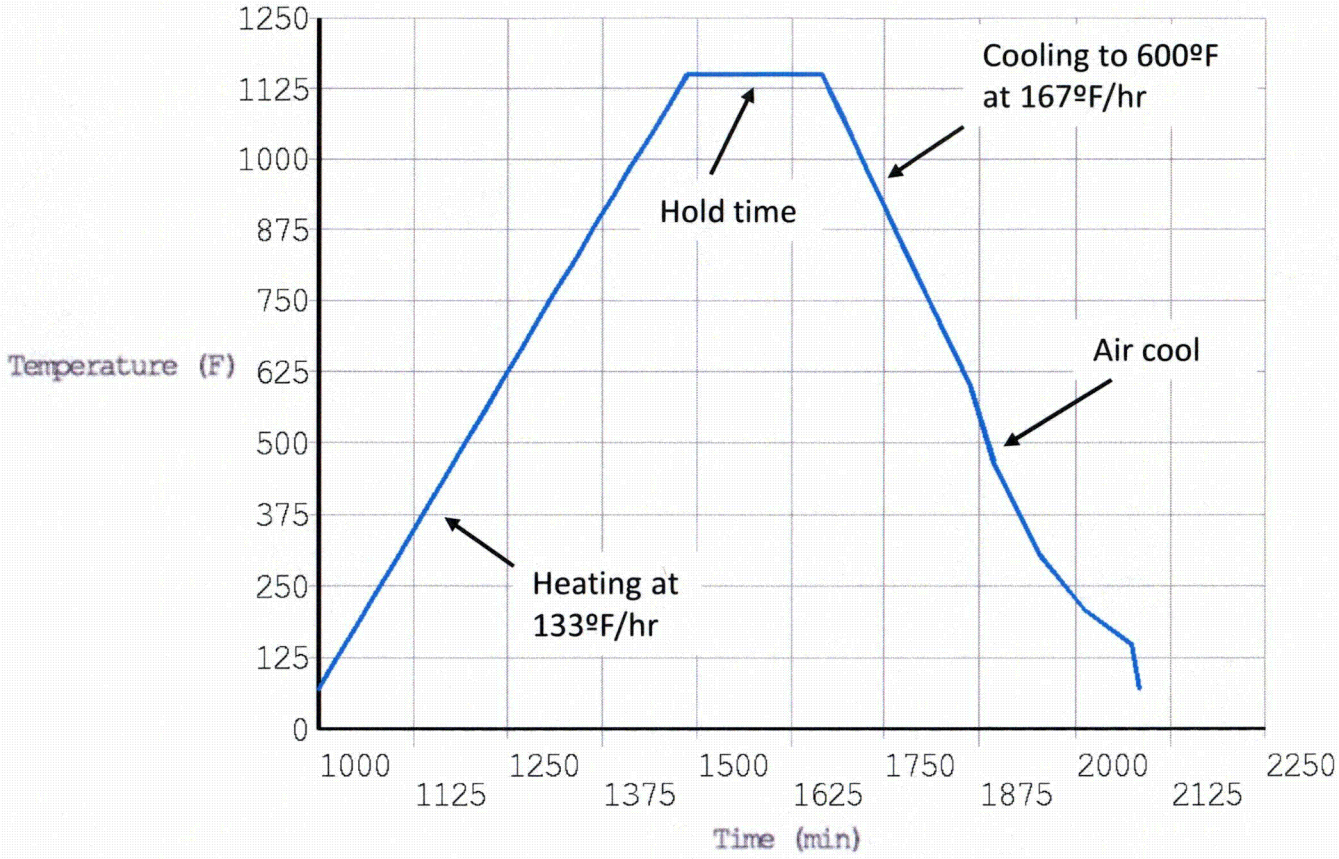

Figure 9: Time vs. Temperature Curve for PWHT

Note:
1. PWHT temperature history is for a typical ID node on the model.

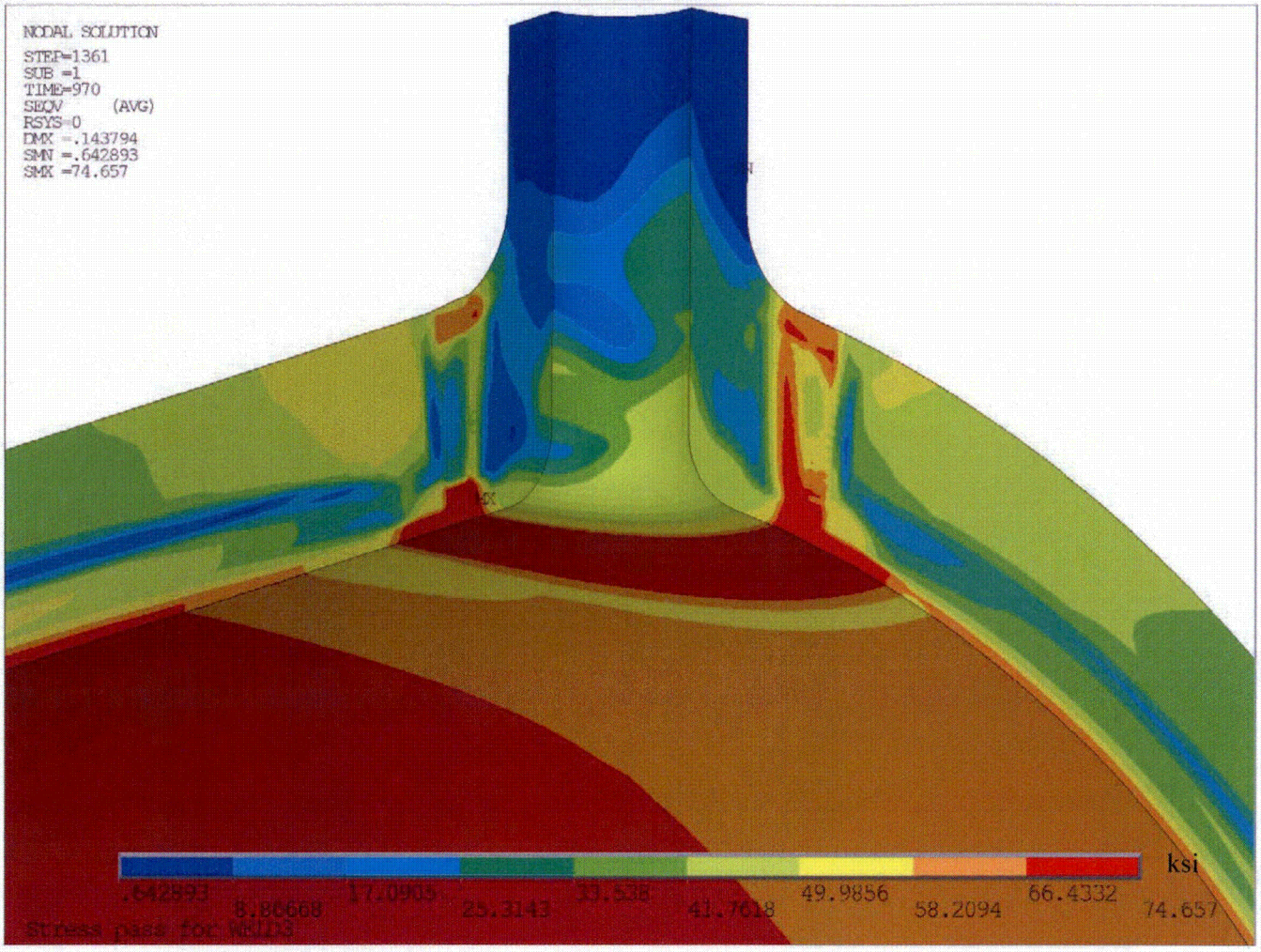

Figure 10: Predicted von Mises Residual Stress at 70°F after ID Patch Weld

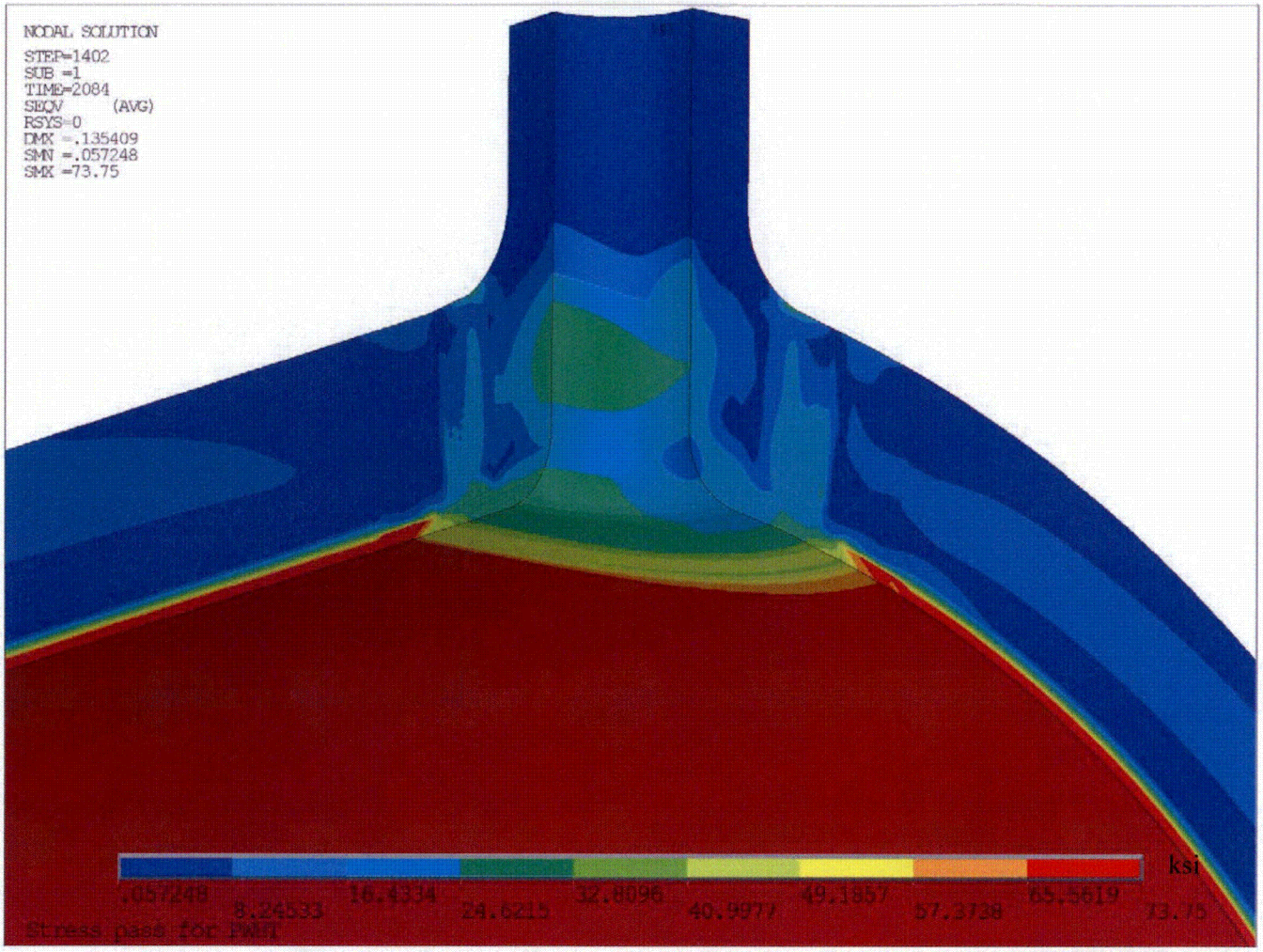

Figure 11: Predicted von Mises Residual Stress at 70°F after PWHT

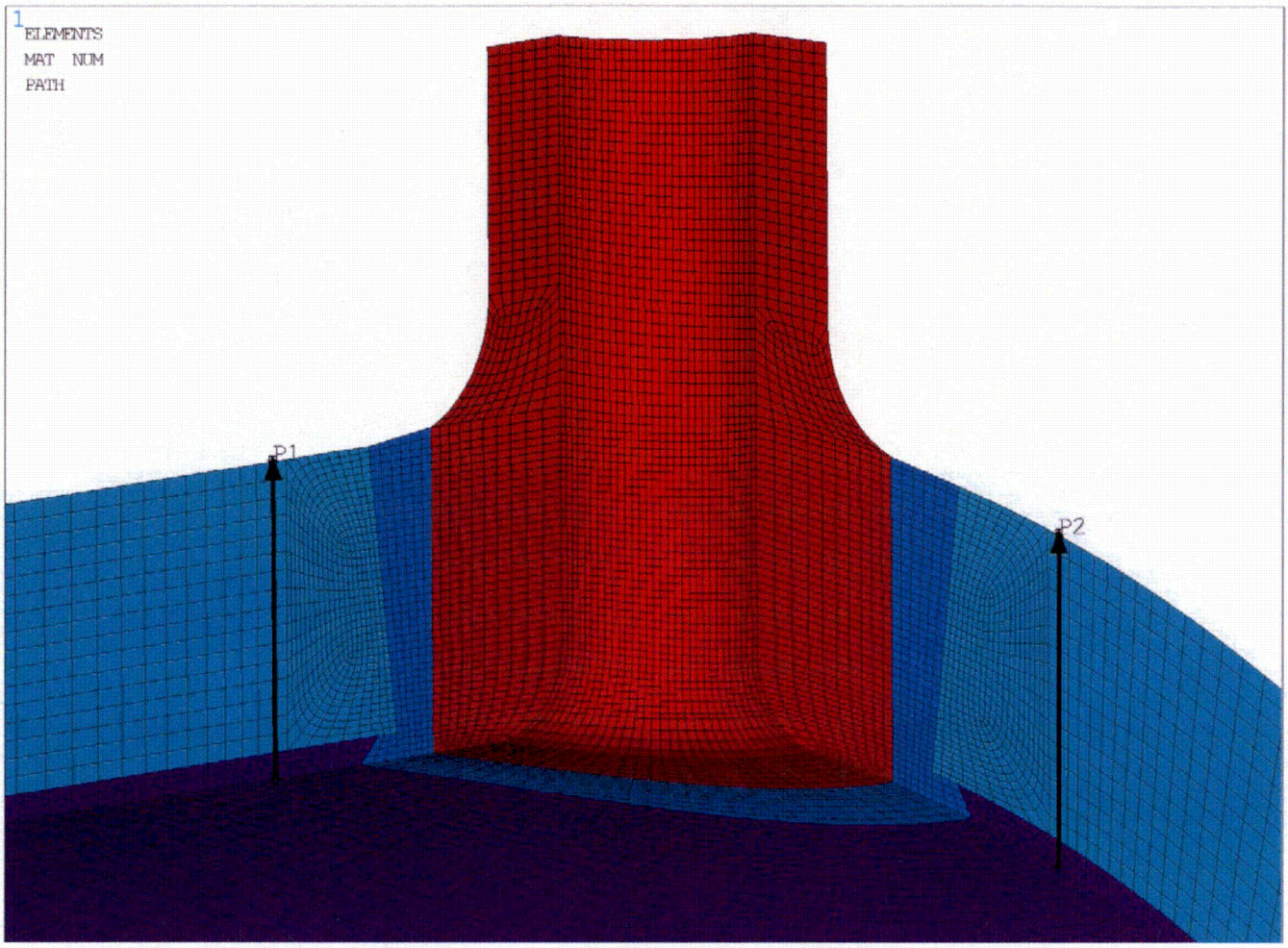

Figure 12: Paths for Stress Extraction

Notes:

1. In the cold leg coordinates, hoop residual stresses along path P1 and axial residual stresses along path P2 are extracted for comparison of before and after PWHT.
2. The before and after PWHT through-wall residual stresses are compared in Figure 13.

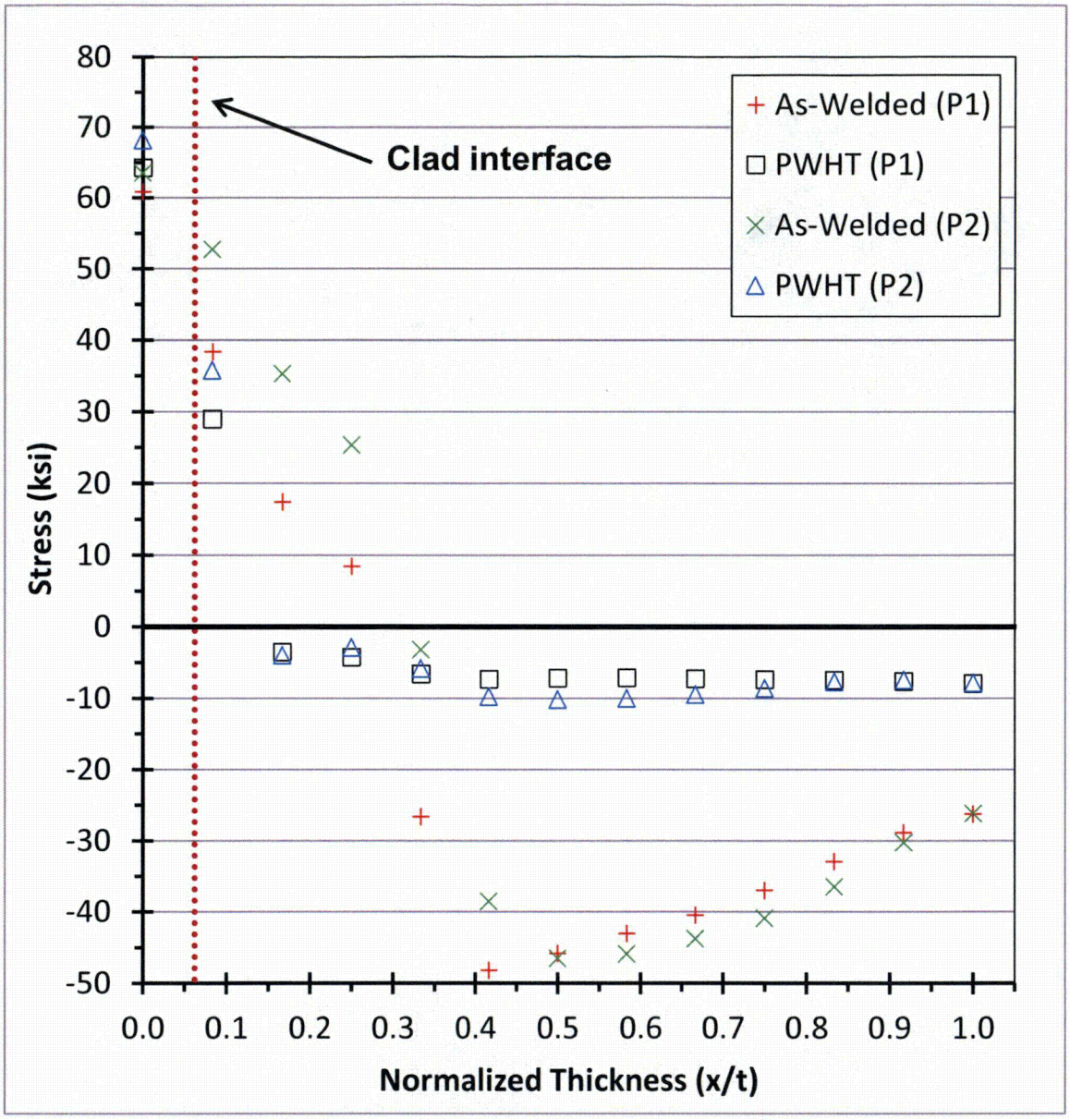

Figure 13: Residual Stress Comparison at 70°F Before and After PWHT

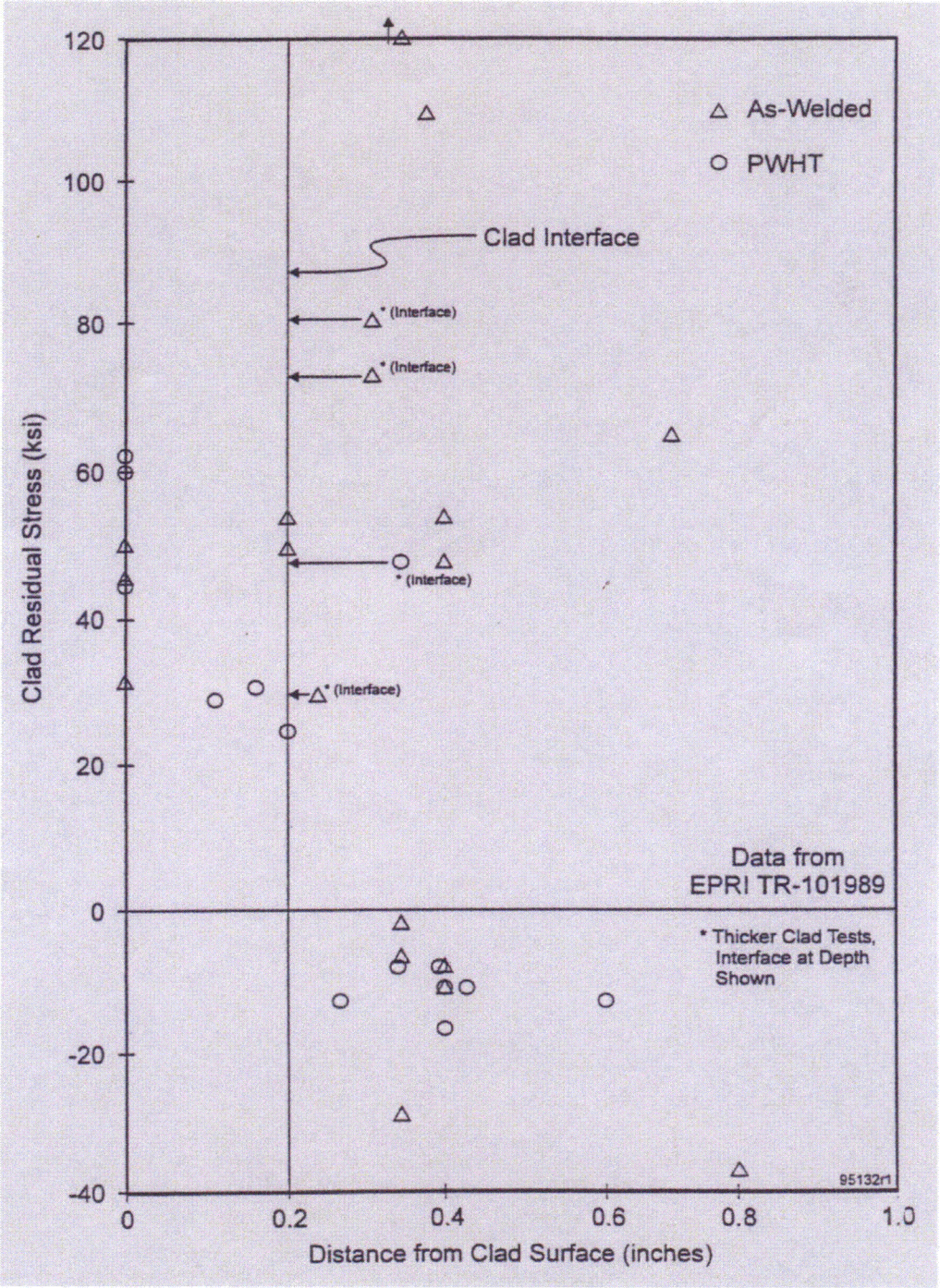

Figure 14: Measured Through-Wall Residual Stresses for PWHT

Notes:
1. Figure is obtained from EPRI report TR-105697 [10].
2. Measurements show little to no stress reduction in the cladding after PWHT.
3. Measurements show significant stress reduction in the base metal after PWHT.

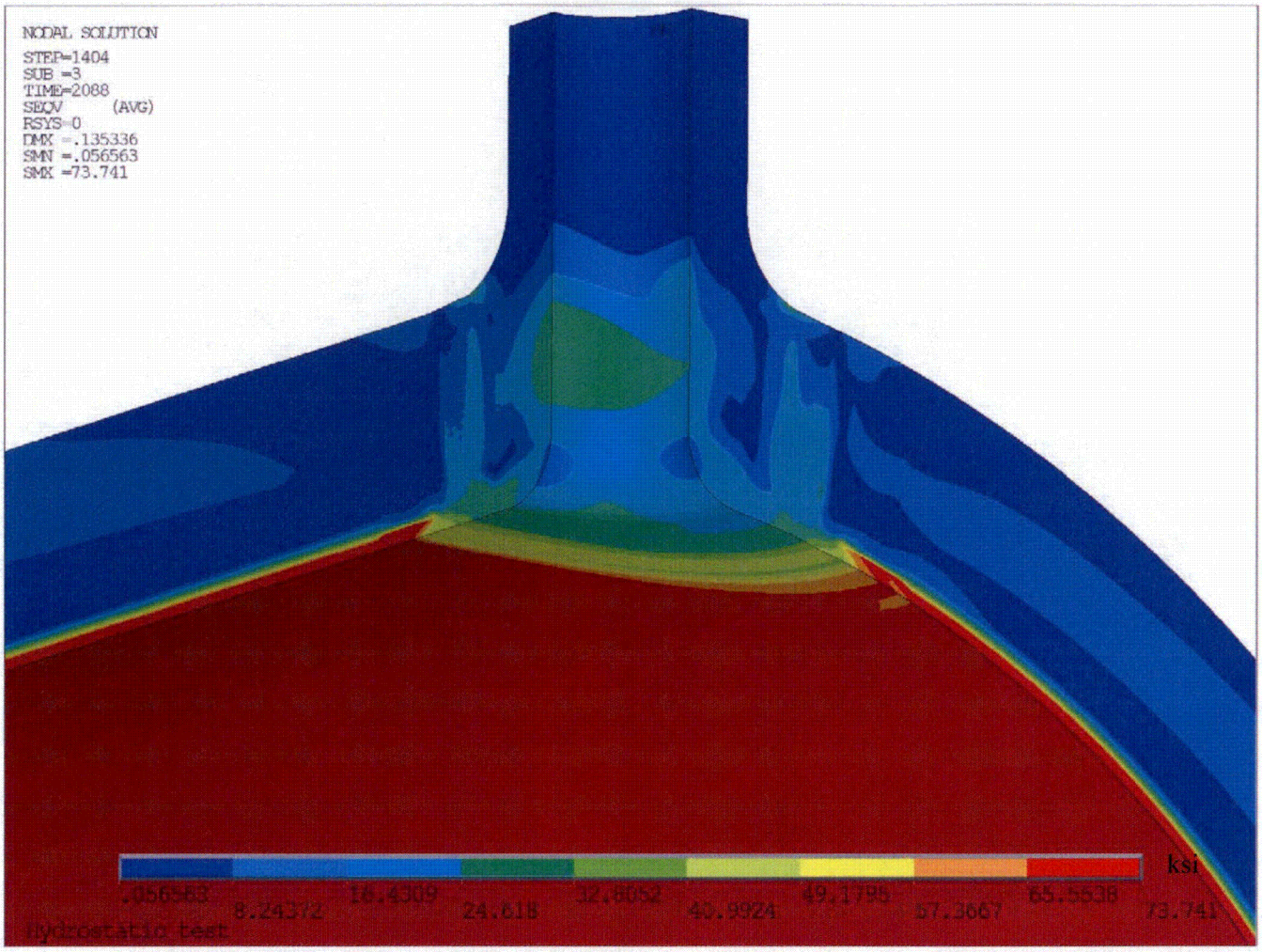

Figure 15: Predicted von Mises Residual Stress at 70°F after Hydrostatic Test

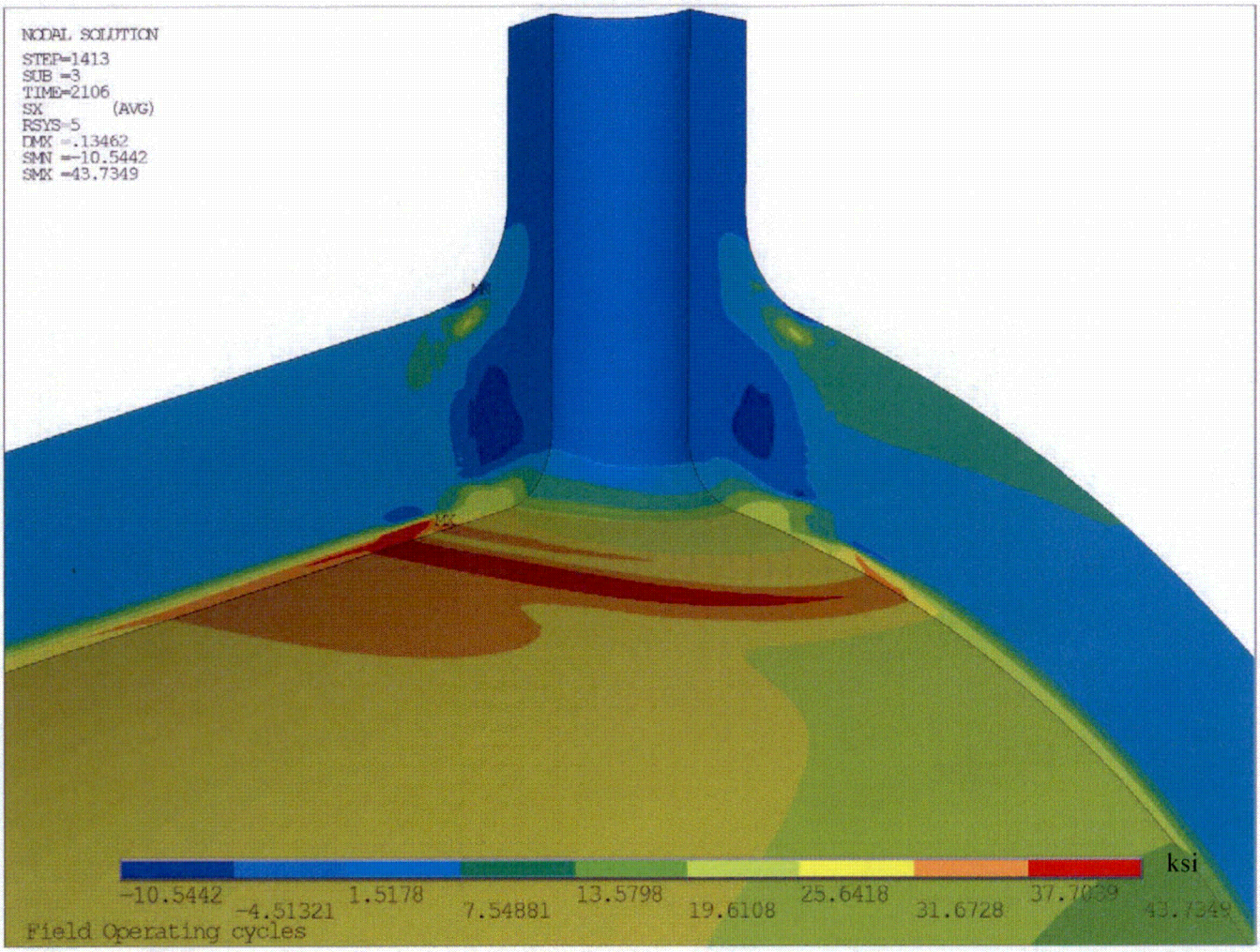

Figure 16: Predicted Radial Residual Stress + Operating Conditions (5th NOC Cycle)

Note:

1. Radial stresses shown in the nozzle axis radial direction.

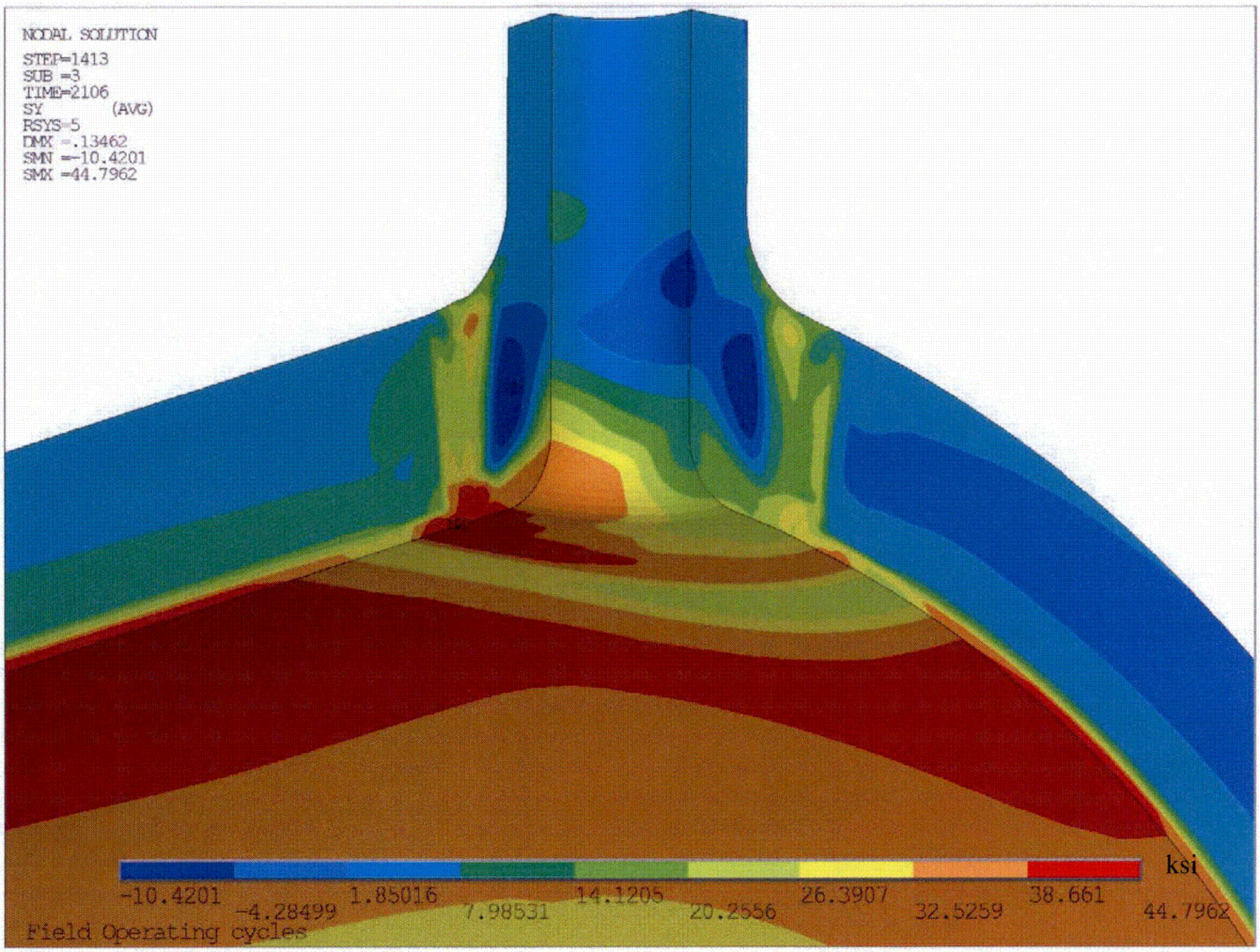

Figure 17: Predicted Hoop Residual Stress + Operating Conditions (5th NOC Cycle)

Note:

1. Hoop stresses shown in the nozzle axis circumferential direction.

APPENDIX A

COMPUTER FILES LISTING

File Name	Description
Palisades_CL.INP	Input file to create base geometry model [1]
MProp_MISO.INP	Elastic-plastic Material properties inputs [1]
Autonugsel.mac	Macro that groups elements into nuggets
BCNUGGET3D.INP	Weld pass and model boundary definition file
THERMAL3D.INP	Input file to perform the thermal pass of welding simulation
THM_PWHT.INP	Input file to perform the thermal pass of PWHT
STRESS3D.INP	Input file to perform the stress pass of welding simulation
CBC.INP	Input file to apply mechanical boundary conditions
THM_PWHT_mntr.inp	Processed thermal pass load steps for PWHT
WELD#_mntr.inp	Processed thermal pass load steps for stress pass # = 1-3
*.mac	WRS analysis macro files required for analysis
THERMAL3D.TXT	Parameter input file for thermal pass of welding simulation
STRESS3D.TXT	Parameter input file for stress pass
GenStress.mac	Macro to extract PWHT stress results
GETPATH.TXT	Through-wall stress path definition to extract PWHT stress results

ATTACHMENT 3

Areva, Inc. letter number AREVA-15-02279,

"Transmittal of Updated Task 6 Letter to Support Palisades Relief Request for PA-MSC-1283,"

dated July 7, 2015

AREVA

July 7, 2015
AREVA-15-02279

Mr. Jim Molkenthin
Program Director
PWROG Materials Committee
16 International Drive
Windsor, CT 06095

Subject: Transmittal of Updated Task 6 Letter to Support Palisades Relief Request for PA-MSC-1283

Reference: PWR Owners Group Project Authorization, PA-MSC-1283R1, Evaluation of Applicable Dissimilar Metal Welds Joining Alloy 600 Branch Connection Nozzles to Primary Loop Piping (B&W Units and Palisades only)

Dear Jim:

Please find attached the updated Task 6 - Letter to Support Palisades Relief Request. AREVA has reviewed the recent structural evaluations performed by Structural Integrity Associates, Inc (SIA). The attached letter report provides the following: 1) a summary of the SIA work methodology and results, 2) assessment of the pedigree of the SIA work analysis, and 3) AREVA's position on the applicability of the SIA work for supporting a relief request.

The subject document is provided as a final deliverable under PA-MSC-1283R1.

If you have any questions or require additional information, please feel free to contact me by phone at (434) 832-2763 or by email at tammy.natour@areva.com.

Best regards,

Tammy Natour

Tammy Natour
Project Manager, NSSS Engineering

AREVA INC
3315 Old Forest Road, Lynchburg, VA 24501
Tel.: (434) 832-3000 - Fax: (434) 832-3840 www.areva.com

Copy with attachment:
William Sims (Entergy)
Larry Theriault (Entergy)
Stephen Davis (Entergy)
Jeff Erickson (Entergy)
Edward Blackard (Entergy)
Brian Haibach (AREVA)
Ryan Hosler (AREVA)
Tim Wiger (AREVA)
Ashok Nana (AREVA)
Tom Riordan (AREVA)
Record's Center L.502238/T1.2

AREVA INC
3315 Old Forest Road, Lynchburg, VA 24501
Tel.: (434) 832-3000 - Fax: (434) 832-3840 www.areva.com

Introduction

The purpose of this letter is to review the Structural Integrity Associates, Inc. (SIA) work performed to evaluate Primary Water Stress Corrosion Cracking (PWSCC) in the hot leg and cold leg branch connection nozzles at Palisades Nuclear Plant (PNP). After completing the review of the SIA work documented in References [1-8], this letter provides the following: 1) a summary of the SIA work methodology and results, 2) assessment of the pedigree of the SIA work analysis, and 3) AREVA's position on the applicability of the SIA work for supporting a subsequent relief request.

Summary of SIA Work

The SIA work postulated circumferential and axial-radial flaws in the Alloy 182 small bore nozzle-to-primary coolant system loop piping weld. The postulated flaws were assumed to initiate at plant startup and grow due to PWSCC. The SIA work performed in References [1-8] included finite element model development, residual stress analysis, crack growth calculation, and flaw stability assessment.

The methodology followed by SIA to demonstrate structural integrity and assure leak tightness of the branch connection nozzle-to- piping weld(s) was consistent with American Society of Mechanical Engineers (ASME) Boiler and Pressure Vessel Code and industry practices. The SIA methodology fulfilled the general requirements of the ASME, Section XI code for evaluating flaws. A typical flaw evaluation per ASME, Section XI involves the following steps:

(a) Determining the configuration and sizes of the bounding flaws.
(b) Determining the normal stresses at the location of the postulated flaw.
(c) Performing a flaw growth analysis to establish the end-of-evaluation-period flaw dimensions.
(d) Determining material properties required for analysis.
(e) Determining the failure mechanism for the end-of-evaluation-period flaw dimensions.
(f) Determining the acceptability of the analyzed components for continued service.

The methodology used for analyzing the assumed PWSCC flaws addressed all the steps listed above as explained in detail in the following text.

The SIA work postulated both circumferential and radial flaws with respect to the nozzle axis for both the hot leg [5] and cold leg branch connection locations [6]. The circumferential flaw was assumed to align with the interface between the boss weld and the nozzle with full (360°) around the circumference length, with analysis performed for initial flaw depths of 0.025" and 0.1" [5 and 6]. In addition, two nozzle radial flaws are postulated with thumbnail shape, one axial with respect to the main loop piping and one circumferential to the main loop piping [5 and 6]. The radial flaws were also considered to have initial depths of 0.025" and 0.1". Reference [9] provided technical and operating experience justification that clearly demonstrates an initial flaw depth of 0.025" is a conservative assumption for the purpose of the crack growth calculations being performed for the Alloy 82/182 full-penetration branch pipe connection weld of the hot-leg drain nozzle at Palisades. Thus, the 0.1" flaw depth used is overly conservative. Reference [9] also added that the assumption of a growing PWSCC flaw present at plant startup is a conservative assumption given the time required for the PWSCC initiation process, especially given the large effect on crack initiation time expected due to the post-weld heat treatment (PWHT) applied to this component.

The SIA work in References [3 and 4] performed detailed finite element analysis (FEA) to determine the residual plus operating stresses normal to the surfaces of the postulated flaws, which were used in the crack growth analysis [5 and 6]. References [3 and 4] simulate all fabrication steps used in the construction of the components including 1) deposit clad on hot leg pipe inside diameter (ID) surface; 2) install nozzle, backing ring, and deposit boss main weld; 3) remove backing ring and deposit ID patch weld; 4) post-weld heat treatment; and 5) hydrostatic testing. After completing the welding

simulation, References [3 and 4] impose 5 cycles of "shake down" with normal operating temperature and pressure. The weld simulations described in References [3 and 4] contain sufficient level of details to reasonably estimate the weld residual stresses. Consistent with industry practices, the material properties and weld parameters were selected to produce a conservative estimation of the residual stresses.

References [5 and 6] performed crack growth analysis to support PWSCC susceptibility concerns at the PNP hot leg to drain nozzle boss weld and bounding cold leg branch connection nozzle, respectively. The PWSCC crack growth analyses in References [5 and 6] were performed using the extracted residual plus operating pressure/temperature stresses from References [3 and 4] as applicable for both circumferential and axial cracks. Additionally, external loads were included by applying a bending moment to the main loop piping. The PWSCC crack growth rates used in References [5 and 6] were from Reference [10], which is accepted throughout the industry as the proper and conservative crack growth rates to be used for analyzing PWSCC flaw growth in Alloy 82/182 welds. The crack growth analyses in References [5 and 6] performed crack growth for both axial and circumferential postulated flaws considering initial crack sizes of 0.025" and 0.1". Stress intensity factors for all flaws were derived by generating explicit flaw FEA models with varying flaw sizes. For the hot leg analysis [5] the axial crack on the 0° plane (radial with respect to nozzle and axial with respect to main loop piping) was found to be limiting, growing from 0.025" to 75% through wall in 30.5 years. For the bounding cold leg nozzle [6], the circumferential flaw (with respect to the nozzle) was found to be limiting, growing from 0.025" to 75% through wall in 55.6 years.

In support of a related prior relief request, Reference [8] performed an analysis to determine acceptability of final flaw sizes in the hot leg drain nozzle using limit load analysis based on ASME Code, Section III, NB-3228.1 [11]. Through wall axial flaws and part-through wall circumferential flaws were modeled in a series of finite element models utilizing elastic-perfectly plastic material properties. Pressure loadings were ramped up until collapse was predicted. It does not appear that any faulted condition bending loads on the pipe were considered. Reference [8] concluded that for part-through wall circumferential flaw and a 100% through wall axial flaw, the hot leg, the hot leg-to nozzle-weld, and the main nozzle body remain structurally stable using the rules of ASME Code, Section III, NB-3228.1 [11].

Summary of Results

Circumferential and Radial (or Axial) Flaws:

The SIA work postulated both circumferential and radial flaws with respect to the nozzle axis. For the hot leg drain nozzle the limiting flaw was found to be the nozzle radial flaw (axial with respect to the hot leg), while for the bounding cold leg branch connection nozzle the circumferential flaw was found to be limiting. Overall, the hot leg radial-axial flaw was limiting in with 30.5 years for a 0.025" crack to grow 75% through wall, compared to the cold leg with 55.6 years to reach 75% through wall.

In terms of years of time during which the reactor is at operating pressure and temperature, or Effective Full Power Years (EFPY), the limiting hot leg flaw has a 1.7 EFPY margin (30.5 EFPY — 28.8 EFPY), where 28.8 is the projected EFPY at end of the next refueling outage (IR25).

Evaluation of SIA Assumptions

The work performed by SIA to support the PNP relief request regarding PWSCC concern for the hot leg drain weld provides a conservative and methodical assessment of the postulated flaw that satisfies flaw evaluation requirements of the ASME code and recommended industry practices. The following is a list of conservative assumptions made in the evaluation:

1. The assumption of a growing PWSCC flaw present at plant startup is a conservative assumption given the time required for the PWSCC initiation process, especially given the large effect on crack initiation time expected due

to the post-weld heat treatment (PWHT) applied to this component. As a supplement to the analysis, Attachment A of Reference [7] estimates that the crack initiation time for the hot leg drain nozzle is approximately 130 years, and over 600 years for the bounding cold leg nozzle. In AREVA's opinion these appear to be best estimates and not lower bounds.

2. The crack growth rates used in the evaluation are conservative. French research investigators have developed a disposition equation that includes a factor of 2 reduction in the crack growth rate as a function of stress intensity factor (K) for Alloy 182 that has been exposed to PWHT [13]. For this full penetration weld configuration, the PWHT was performed after the weld repair was made [14].

AREVA Position

AREVA has reviewed the work performed by SIA in References [1-8]. The SIA work followed ASME code and recommended industry practices. It is AREVA's opinion based on reviewing the SIA work in References [1-8], that the assumptions supporting an estimated 30.5 EFPY for a PWSCC crack to reach 75% through wall are appropriate. Two conservatisms exist, as mentioned above. The cost and benefit of removing these conservatisms is unknown at this time. If the above two estimates of the conservatisms in crack initiation time and crack growth rate are considered, it would take approximately 191 years for the hot leg flaw to reach 75% through wall (i.e., 130 years for initiation plus 2×30.5 years for growth), and would just exceed 200 years to reach 95% through wall. Considering these conservatisms for the cold leg, the time to reach 75% through wall would be greater than 600 years. The SIA work shows that an axial flaw in the hot leg is more likely to initiate and grow through wall compared to other locations and flaw orientations. For this configuration, axial flaws would not lead to catastrophic failure due to RCS leakage monitoring per WCAP-16465, "Pressurized Water Reactor Owners Group Standard RCS Leakage Action Levels and Response Guidelines for Pressurized Water Reactors" [15], as well as the enhanced leakage monitoring program [16]. Together with leakage monitoring, the Palisades Technical Specifications would identify subsequent leakage well in advance of potential safety issues. Therefore, Bare Metal Visual (BMV) examination is sufficient to ensure that cracking in the hot and cold leg nozzles do not pose an immediate safety concern for PNP.

References

1. Structural Integrity Associates, Inc., Calculation 1400669.310, *Finite Element Model for Hot Leg Drain Nozzle*, Revision 0.
2. Structural Integrity Associates, Inc., Calculation 1400669.320, *Finite Element Model Development for the Cold Leg Drain, Spray, and Charging Nozzles*, Revision 0.
3. Structural Integrity Associates, Inc., Calculation 1400669.312, *Hot Leg Drain Nozzle Weld Residual Stress Analysis*, Revision 0.
4. Structural Integrity Associates, Inc., Calculation 1400669.322, *Cold Leg Bounding Nozzle Weld Residual Stress Analysis*, Revision 0.
5. Structural Integrity Associates, Inc., Calculation 1400669.313, *Crack Growth Analysis of the Hot Leg Drain Nozzle*, Revision 0.
6. Structural Integrity Associates, Inc., Calculation 1400669.323, *Crack Growth Analysis of the Cold Leg Bounding Nozzle*, Revision 0.
7. Structural Integrity Associates, Inc., Report 1400669.401, *Evaluation of the Palisades Nuclear Plant Branch Line Nozzles for Primary Water Stress Corrosion Cracking*, Revision 0.
8. Structural Integrity Associates, Inc., Calculation 1200895.308, *Hot Leg Drain Nozzle Limit Load Analyses for Flawed Nozzle-to-Hot Leg Weld*, Revision 0.
9. Dominion Engineering, Inc., Letter L-4199-00-02, Rev. 0, *Initial Flaw Assumption for Alloy 82/182 Full-Penetration Branch Pipe Connection Weld at Palisades*, dated March 9, 2014.
10. *Materials Reliability Program Crack Growth Rates for Evaluating Primary Water Stress Corrosion Cracking (PWSCC) of Alloy 82, 182, and 132 Melds (MRP-115NP)*, EPRI, Palo Alto, CA: 2004. 1006696.

11. ASME Boiler and Pressure Vessel Code, Section III, Rules for Construction of Nuclear Facility Components, 2001 Edition with Addenda through 2003.
12. ASME Boiler and Pressure Vessel Code, Section XI, Rules for Inservice Inspection of Nuclear Plant Components, 2001 Edition with Addenda through 2003.
13. Letter from G. White (Dominion Engineering, Inc.) to W. Sims (Entergy), "*Effect of Post-Weld Heat Treatment Applied to Alloy 82/1 82 Full-Penetration Branch Pipe Connection Welds at Palisades*," DEI Letter L-4199-00-01, Rev. 0, dated February 25, 2014.
14. Entergy Nuclear Operations, Inc. letter PNP 2014-029, *Response to Third Request for Additional Information dated March 5, 2014, for Relief Request RR 4-18 – Proposed Alternative , Use of Alternate ASME Code Case N-770-1 Baseline Examination*, dated March 6, 2014.
15. Westinghouse Electric Company, WCAP-16465, Rev. 0, Non-Proprietary, "*Pressurized Water Reactor Owners Group Standard RCS Leakage Action Levels and Response Guidelines for Pressurized Water Reactors*," dated September 2006.
16. NRC Letter with Safety Evaluation for Relief Request RR 4-18, *Palisades Nuclear Plant – Proposed Alternative, Use of Alternate ASME Code Case N-770-1 Baseline Examination (Tac No. MF3508)*, dated September 4, 2014 (ML14223B226).